Theoretical Analysis of the CH Stretching Overtone Vibration of 1,2-Dichloroethylene

Kaito Takahashi, Michihiko Sugawara, and Satoshi Yabushita*

Department of Chemistry, Faculty of Science and Technology, Keio University, 3-14-1 Hiyoshi, Kohoku-ku, Yokohama 223-8522, Japan

Received: September 13, 2001; In Final Form: November 29, 2001

The intensity of the CH stretching overtone spectra of liquid *cis*-dichloroethylene is known to be greater than that of the trans isomer, even though the transition energies are almost the same. To obtain theoretical insight on this feature, we performed a vibrational calculation under the local mode model, which is preferred for describing vibration of light−heavy bonds, using the grid method and the potential energy surface (PES) and the dipole moment function (DMF) calculated by hybrid density functional theory method. It was determined that the DMF, in the direction perpendicular to the CC bond, was significantly distorted from linearity as a function of the CH bond length. This distortion, which is regarded as the electric anharmonicity, was greater for the cis isomer, thus giving a stronger overtone absorption intensity for this isomer. In addition, the numerical accuracy in representing the PES and DMF was discussed for the overtone vibrational calculation.

1. Introduction

For the calculation of the intensities of vibrational transitions, both the vibrational wave function and the dipole moment function (DMF) are essential issues. For the fundamental transitions, the intensities are readily derived from the ab initio potential energy surface (PES) and the ab initio DMF under the harmonic approximation using normal coordinates.

In treating stretching overtone vibration of molecules with XH bonds, where X = C,O and so on, the local mode model, in which the vibrational wave function is described as a product of anharmonic oscillators using internal coordinates, has shown great success.[1−4] Kjaergaard et al. have used the harmonic coupled anharmonic oscillator (HCAO) model to predict the transition energies and the intensities of several simple molecules such as H_2O, H_2O_2, NH_3, and CH_2O.[5,6] In their calculation, the parameters of their vibrational wave function, a product of Morse oscillators, were determined from the fit to the observed peak positions, while the intensities were calculated from the DMF obtained by fitting the calculated ab initio dipole moment derivatives around the equilibrium structure to a series of expansions in the displacement coordinates. Recently, they calculated the CH overtone spectra of naphthalene, anthracene, and their cations by using Morse parameters obtained from ab initio calculation.[7] However, overtone vibration calculations using both PES and DMF determined from ab initio calculations are still very rare.

Upon examining the vibrational spectra of several representative liquid hydrocarbons with various kinds of CH oscillators, Burberry et al. suggested a "universal intensity concept": for a given CH stretching overtone transition, a single absorption cross section per CH oscillator, regardless of type, could account for the observed spectral intensity at quantum levels $v = 3$, 4, 5, and 6.[8] However, overtone spectra of liquid *cis*- and *trans*-dichloroethylene measured by use of a photon-counting absorbance spectrophotometer[9,10] by Okada, Yamamoto, and Tsubomura showed results in contradiction to this concept.[11] The integrated intensities of the cis isomer were greater than those of the trans isomer by a factor of 1.5−2.0.

The present work is intended to obtain further insight on this curious experimental result. It is expected that a simple local mode model, in which the XH vibration is described by a single anharmonic oscillator, would be sufficient for the calculation of the CH vibration in 1,2-dichloroethylene. This is because the two CH bonds with high stretching frequency are on different atoms; thus, the effect of the coupling between these two CH bonds and with other parts of the molecule can be very small. Because the integrated intensities of overtones are very sensitive to the vibrational wave function and the DMF, to fully incorporate the ab initio results, we obtained the one-dimensional vibrational states by numerically solving the Schrödinger equation. Vibrational calculation using the grid method was performed on the PES and DMF calculated by the ab initio method. Because past calculations on this feature showed the need of electron correlation,[12] we used the hybrid density functional theory (DFT) method. It has already been reported that the hybrid functionals produce results as good as the MP2 method for fundamental frequencies.[13] In this way, this can be a test on the applicability of the hybrid functionals at elongated bond lengths.

Moreover, we must consider the fact that the experimental results are for the liquid phase. The Onsager model[14] has been used to incorporate solvation effects into ab initio calculation[15−17] in the form of the self-consistent reaction field (SCRF) method. Further modifications to this theory have been used for the accurate calculation of the fundamental frequency and intensity for dilute solutions.[18] We investigated the applicability of the SCRF method for calculating the overtone intensities of pure liquid.

In recent atmospheric studies, the absorption of overtone bands of OH stretching modes is being investigated with great interest.[19−21] For example, overtone absorption by water clusters is thought to account for the difference between the observed and the modeled absorption of sun light by the atmosphere. However, obtaining the experimental absorption intensity for each cluster, for example, dimer, trimer and so on, is difficult.

* To whom correspondence should be addressed. E-mail: yabusita@chem.keio.ac.jp. Fax: +81-45-566-1697.

10.1021/jp0135252 CCC: $22.00
Published on Web 02/19/2002

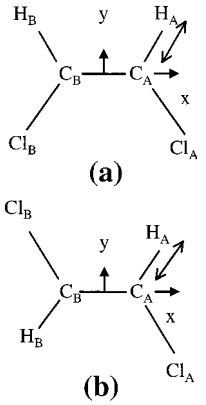

Figure 1. Schematic diagram of (a) *cis*- and (b) *trans*-dichloroethylene and the atom labeling used in this paper. The *x* coordinate was taken along the CC bond, while the *y* coordinate was taken perpendicular to the CC bond. The origin was taken at the center of the CC bond. The variation of the bond distance was considered to be on the C_AH_A bond.

Furthermore, one of the sources of atmospheric radicals in low-light conditions has been reported to be overtone-initiated photodissociation processes.[21] Thus, the knowledge of accurate absorption intensities on these transitions is key to accessing the significance of these processes in the atmosphere. With the intent to apply the present vibrational calculation method to those problems in our future study, the numerical efficiency and accuracy of the grid method were examined. Because several recent theoretical calculations on overtone intensities have used PES and DMF obtained by fitting ab initio data onto analytical functions,[7,22,23] we examined particularly the sensitivity of the vibrational calculation results on the incorporation method of the ab initio data.

2. Theory and Computational Method

2.1. Simple Local Mode Model. Under the local mode model, the CH stretching part of the vibrational wave function of 1,2-dichloroethylene is written as a product of two one-dimensional wave functions, namely,

$$\psi_i(r_1)\psi_j(r_2) \quad \text{or} \quad \psi_j(r_1)\psi_i(r_2) \tag{1}$$

where r_1 and r_2 are the CH bond length coordinates, and i and j stand for the quantum numbers. Because these product wave functions in local mode do not reflect the molecular symmetry, it should be symmetry-adapted.[24] Considering *cis*-dichloroethylene (C_{2v}), for example, the following symmetry adapted linear combination would be expected for $i \neq j$

$$\Psi^{A_1}(r_1,r_2) = \frac{1}{\sqrt{2}}\{\psi_i(r_1)\psi_j(r_2) + \psi_j(r_1)\psi_i(r_2)\} \tag{2}$$

$$\Psi^{B_1}(r_1,r_2) = \frac{1}{\sqrt{2}}\{\psi_i(r_1)\psi_j(r_2) - \psi_j(r_1)\psi_i(r_2)\} \tag{3}$$

and for $i = j$

$$\Psi^{A_1}(r_1,r_2) = \psi_i(r_1)\psi_i(r_2). \tag{4}$$

As for *trans*-dichloroethylene (C_{2h}), the labeling of the representation in the above wave functions should be changed as follows: $A_1 \rightarrow A_g$, $B_1 \rightarrow B_u$.

The coordinates are taken so that they belong to symmetry species of the molecule, as seen in Figure 1. Considering the cis isomer, once again, the *x* and *y* components of the dipole moment function have the following symmetry property:

$$\mu_x(r_1,r_2) = -\mu_x(r_2,r_1) \qquad (B_1) \tag{5}$$

$$\mu_y(r_1,r_2) = \mu_y(r_2,r_1) \qquad (A_1) \tag{6}$$

The v quantum excited states from the zero-point vibration state ($\Psi_0(r_1,r_2) = \psi_0(r_1)\psi_0(r_2)$), expected to account for the overtone intensity, are

$$\Psi_v^{A_1}(r_1,r_2) = \frac{1}{\sqrt{2}}\{\psi_v(r_1)\psi_0(r_2) + \psi_0(r_1)\psi_v(r_2)\} \tag{7}$$

and

$$\Psi_v^{B_1}(r_1,r_2) = \frac{1}{\sqrt{2}}\{\psi_v(r_1)\psi_0(r_2) - \psi_0(r_1)\psi_v(r_2)\} \tag{8}$$

Thereby, the transition moment between Ψ_0 and $\Psi_v^{B_1}$ is

$$\langle\Psi_0|\hat{\mu}_x|\Psi_v^{B_1}\rangle = \frac{1}{\sqrt{2}}\int\int\psi_0(r_1)\psi_0(r_2)\mu_x(r_1,r_2)[\psi_v(r_1)\psi_0(r_2) - \psi_0(r_1)\psi_v(r_2)]\,dr_1\,dr_2 \tag{9}$$

$$= \frac{1}{\sqrt{2}}[\int\int\psi_0(r_1)\psi_0(r_2)\mu_x(r_1,r_2)\psi_v(r_1)\psi_0(r_2)\,dr_1\,dr_2 - \int\int\psi_0(r_1)\psi_0(r_2)\mu_x(r_1,r_2)\psi_0(r_1)\psi_v(r_2)\,dr_1\,dr_2] \tag{10}$$

In the second integration, the bond coordinates are exchanged

$$\int\int\psi_0(r_1)\psi_0(r_2)\mu_x(r_1,r_2)\psi_0(r_1)\psi_v(r_2)\,dr_1\,dr_2 = \int\int\psi_0(r_2)\psi_0(r_1)\mu_x(r_2,r_1)\psi_0(r_2)\psi_v(r_1)\,dr_2\,dr_1 = \int\int\psi_0(r_1)\psi_0(r_2)[-\mu_x(r_1,r_2)]\psi_v(r_1)\psi_0(r_2)\,dr_1\,dr_2 \tag{11}$$

thus yielding

$$\langle\Psi_0|\hat{\mu}_x|\psi_v^{B_1}\rangle = \frac{1}{\sqrt{2}} \times 2\int\int\psi_0(r_1)\psi_0(r_2)\mu_x(r_1,r_2) \times \psi_v(r_1)\psi_0(r_2)\,dr_1\,dr_2 = \sqrt{2}\int\psi_0(r_1)\mu'_x(r_1)\psi_v(r_1)\,dr_1 \tag{12}$$

where

$$\mu'_x(r_1) = \int\psi_0(r_2)\mu_x(r_1,r_2)\psi_0(r_2)\,dr_2 \tag{13}$$

In the present calculation, as usual, we assume the following equation:

$$\mu'_x(r_1) \equiv \mu_x(r_1,r_{2\text{eq}}) \tag{14}$$

namely, the expectation value of the second CH bond distance r_2 in the ground vibrational state is equal to the one at the potential minimum. Therefore, the two-dimensional integration of the transition moment becomes a one-dimensional integration of

$$\langle\Psi_0|\hat{\mu}_x|\Psi_v^{B_1}\rangle = \sqrt{2}\int\psi_0(r_1)\mu_x(r_1,r_{2\text{eq}})\psi_v(r_1)\,dr_1 \tag{15}$$

In the same way, we have

$$\langle \Psi_0|\hat{\mu}_y|\Psi_v^{A_1}\rangle = \sqrt{2}\int \psi_0(r_1)\mu_y(r_1,r_{2eq})\psi_v(r_1)\,dr_1 \quad (16)$$

As for the trans isomer (C_{2h}), the x and y components of the DMF have the following symmetry property:

$$\mu_x(r_1,r_2) = -\mu_x(r_2,r_1) \qquad (B_u) \quad (17)$$

$$\mu_y(r_1,r_2) = -\mu_y(r_2,r_1) \qquad (B_u) \quad (18)$$

Thereby, the transition moment between Ψ_0 and $\Psi_v^{A_g}$ is zero, and the transition moment between Ψ_0 and $\Psi_v^{B_u}$ has two components:

$$\langle \Psi_0|\hat{\mu}_x|\Psi_v^{B_u}\rangle = \sqrt{2}\int \psi_0(r_1)\mu_x(r_1,r_{2eq})\psi_v(r_1)\,dr_1 \quad (19)$$

$$\langle \Psi_0|\hat{\mu}_y|\Psi_v^{B_u}\rangle = \sqrt{2}\int \psi_0(r_1)\mu_y(r_1,r_{2eq})\psi_v(r_1)\,dr_1 \quad (20)$$

In summary, the transition moment is obtained from the ab initio DMF calculated by varying one CH bond distance while keeping the other at the equilibrium length.

Because the $\Psi_v^{A_1}$ and $\Psi_v^{B_1}$ states for the cis isomer are almost degenerate and cannot be distinguished experimentally, we calculated the sum of the integrated absorption coefficient (km mol^{-1}) for both states, given by

$$A = \ln 10\int \epsilon(\tilde{\nu})\,d\tilde{\nu} = \frac{8N_A\pi^3}{300\,000hc}|\mu_{0v}|^2\tilde{\nu}_{0v} = 2.506\,639\,488|\mu_{0v}|^2\tilde{\nu}_{0v} \quad (21)$$

where $\epsilon(\tilde{\nu})$ is the molar extinction coefficient, $\tilde{\nu}_{0v}$ is the transition energy in cm^{-1} and $|\mu_{0v}|^2$ is the sum of the squared transition moment of the x and y component in debye^2 units. From the discussion above, for both cis and trans isomers, we deduce the following equation using the simple local mode model.

$$A = 2.506\,639\,488 \times 2 \times \{[\int \psi_0(r_1)\mu_x(r_1,r_{2eq})\psi_v(r_1)\,dr_1]^2 + [\int \psi_0(r_1)\mu_y(r_1,r_{2eq})\psi_v(r_1)\,dr_1]^2\} \times \tilde{\nu}_{0v} \quad (22)$$

One would notice that the factor of 2 in front corresponds to the fact that the total absorbance would become twice the absorption of one CH bond. The values of the integrated absorption coefficient, A, which is given using the units km mol^{-1} throughout this paper, can be converted to the units cm molecule^{-1} and to dimensionless oscillator strengths by 1.66 $\times$ 10^{-19} cm molecule^{-1} mol km^{-1} $\times$ A and 1.87 $\times$ 10^{-7} mol km^{-1} $\times$ A, respectively.

2.2. Grid Method for Vibrational Calculation. All of the following vibration calculations were performed using the grid variational method,[25−27] in which the wave function is treated as a discrete sum,

$$|\psi_v\rangle = \sum_{i=1}^{\text{grid}} \psi_v(r_i)|r_i\rangle \quad (23)$$

where $r_i = r_{min} + (i-1)\Delta r$. In the present calculation, we used $r_{eq} - 0.94$ bohr for r_{min} and 0.01 bohr for the separation between each grid point, Δr. In total, 246 grid points were taken between the range of $r_{eq} - 0.94$ bohr($r_{eq} - 0.5$ Å) to $r_{eq} + 1.51$ bohr(r_{eq} + 0.8 Å). We consider the Schrödinger equation for one-dimensional molecular vibration

$$H\psi_v(r) = \left[-\frac{\hbar^2}{2m}\frac{d^2}{dr^2} + V(r)\right]\psi_v(r) = E_v\psi_v(r) \quad (24)$$

where m and $V(r)$ are the reduced mass and the potential function (PES), respectively. The matrix element of the kinetic energy operator has a banded form and is calculated by the finite difference approximation.[25−27] From the fifth-order finite difference approximation, the second derivative of $|r_i\rangle$ is given as

$$\frac{d^2}{dr^2}|r_i\rangle = \frac{1}{\Delta r^2}\left[\frac{-5269}{1800}|r_i\rangle + \frac{5}{3}|r_{i\pm1}\rangle + \frac{-5}{21}|r_{i\pm2}\rangle + \frac{5}{126}|r_{i\pm3}\rangle + \frac{-5}{1008}|r_{i\pm4}\rangle + \frac{1}{3150}|r_{i\pm5}\rangle\right] \quad (25)$$

The potential energy matrix is a diagonal matrix, where the matrix element is the potential energy at each grid point. These values are obtained by sixth-order divided difference interpolation[28,29] of the 16 ab initio single-point calculation results described in section 2.4. This was done by the "Interpolation-[data]" function built in the *Mathematica* program. Following the diagonalization of the Hamiltonian matrix, the eigenvector elements of the v-th state, $\psi_v(r_i)$, are used to calculate the one-dimensional transition moment in eq 22. The DMF matrix becomes a diagonal matrix, just like the PES matrix above. Thus,

$$\langle \psi_0|\hat{\mu}|\psi_v\rangle = \sum_i^{\text{grid}} \psi_0(r_i)\cdot\mu(r_i)\cdot\psi_v(r_i) \quad (26)$$

Once again the values at each grid point are obtained from the interpolation of the 16 ab initio single-point results. All of the vibrational calculations were done on the *Mathematica* program.

2.3. Self-Consistent Reaction Field Method. In this model, the solute is placed in a cavity, which is immersed in a continuous medium with a dielectric constant ϵ. In the present calculation, we will take a sphere with a radius of a as the cavity. The dipole moment of the solute will give an induced dipole in the medium, and the electric field applied to the solute by the solvent, the reaction field, will in turn interact with the dipole of the solute, and lead to net stabilization. In the ab initio theory, this solvent effect is taken in as an external field. With the use of the Onsager model,[14] the reaction field is written as

$$\frac{2(\epsilon-1)}{2\epsilon+1}\frac{\mu}{a^3} \quad (27)$$

This is included into the ab initio calculation by adding a term to the original Fock matrix, F_{ij}^0,[15]

$$F_{ij} = F_{ij}^0 - \frac{2(\epsilon-1)}{2\epsilon+1}\frac{\mu}{a^3}\langle i|\hat{\mu}|j\rangle \quad (28)$$

and is calculated until self-consistency is reached. One should note that if the molecule in the cavity has a dipole moment of zero, the reaction field would be zero. To perform this calculation two parameters, a and ϵ, must be prepared.

2.4. Ab Initio Calculation. All of the ab initio calculations were performed on the Gaussian 98[30] program. Throughout this paper, bond lengths are given in angstroms, bond angles in degrees, and dipole moments in debye. Calculations on 1,2-dichloroethylene were performed by the B3PW91[31,32] and the B3LYP functionals[31,33] using the aug-cc-pVTZ[34−36] basis set

TABLE 1: Calculated and Experimental Geometry of 1,2-Dichloroethylene

Cis Isomer

	calcd			exptl	
	B3PW91 gas	B3PW91 liq	B3LYP gas	ED[a]	MW[b]
CH, Å	1.081	1.081	1.079	1.096	1.100
CCl, Å	1.716	1.717	1.728	1.717	1.717
CC, Å	1.325	1.324	1.324	1.337	1.319
∠CCH, deg	120.4	120.5	120.6	120.3	123.2
∠CCCl, deg	125.1	125.0	125.3	124.0	124.2

Trans Isomer

	calcd		exptl	
	B3PW91 gas	B3LYP gas	ED[a]	IR[c]
CH, Å	1.080	1.078	1.092	1.078
CCl, Å	1.725	1.738	1.725	1.740
CC, Å	1.322	1.321	1.332	1.305
∠CCH, deg	123.8	124.1	124.0	125.3
∠CCCl, deg	121.6	121.6	120.8	119.9

[a] Electron diffraction taken from ref 42. [b] Microwave spectroscopy taken from ref 43. [c] Infrared spectroscopy taken from ref 44.

built in the program. It was found that the vibration calculations using smaller basis sets, such as 4-31G**[37,38] and 6-311G,[39,40] with B3PW91 functional gave almost the same results for the excitation energy but not for the absorption intensity. The optimization was done using the OPT=VTIGHT keyword, while the cavity radius used for the Onsager model calculation (SCRF=DIPOLE keyword) was obtained by using the VOLUME keyword at the optimized geometry. The SCRF method calculations were done using only the B3PW91 functional. For the cavity radii, we used the calculated values of 3.74 for cis isomer and 3.64 for trans isomer. As for the dielectric constant, the experimental values of 9.20[41] and 2.14[41] were used for cis and trans isomers, respectively. The values used for calculating the PES and DMF were obtained by performing single-point calculations for every 0.1 CH bond length, between the regions $r_{eq} - 0.5$ to $r_{eq} + 0.8$ and adding two points, $r_{eq} - 0.05$ and $r_{eq} + 0.05$ around the equilibrium region. Later, we will see that this region is wide enough for the calculation of overtone vibration spectra.

3. Results and Discussions

For the following discussion, we will mainly use the results of the B3PW91 calculation and report the B3LYP results simply in tables. The simple ab initio calculation will be referred to as the gas-phase calculation, while the SCRF calculations will be referred to as the liquid-phase calculation.

3.1. Optimized Geometry. We first discuss the optimized structures of the two isomers. As shown in Table 1, we see good agreement with the experimental values.[42−44] Another feature to test the accuracy of the ab initio calculation is the so-called "cis effect",[45,46] the effect where the cis isomer is more stable than the trans isomer for dihaloethylenes. By studying the equilibrium constant over a temperature range and correcting for the rotational and vibrational energies, Craig et al. obtained a value of 0.72 kcal mol^{-1} for the difference between the minima of the potential energy surface of the two 1,2-dichloroethylene isomers.[45] The calculated energy difference was 0.35 kcal mol^{-1} in favor of cis using the B3PW91 functional and 0.22 kcal mol^{-1} for the B3LYP. Another criterion for accuracy is the dipole moment of the cis isomer, which was calculated to be 1.85 (B3PW91) and 1.88 (B3LYP), while the experimental value is 1.9.[41] Therefore, one can say that the gas-phase ab initio calculation, at least at the equilibrium structure, is accurate. The proper description of the dipole moment is essential not only for the intensity of the overtone spectra but also for an accurate SCRF calculation, because it is directly incorporated into the calculation of the reaction field.

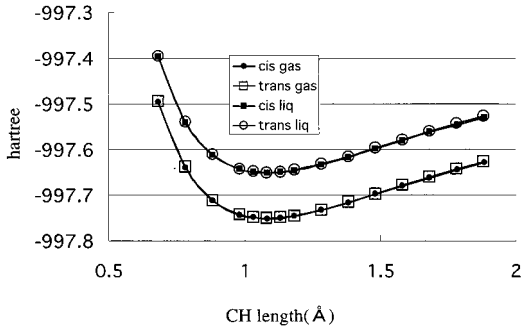

Figure 2. The gas-phase potential energy surface (B3PW91/aug-cc-pVTZ) of *cis*- and *trans*-dichloroethylene. The liquid-phase potential energy surface (B3PW91/aug-cc-pVTZ, SCRF = DIPOLE) is shifted by adding 0.1 hartree. Markers for the cis isomer are shaded while those for the trans isomer are open.

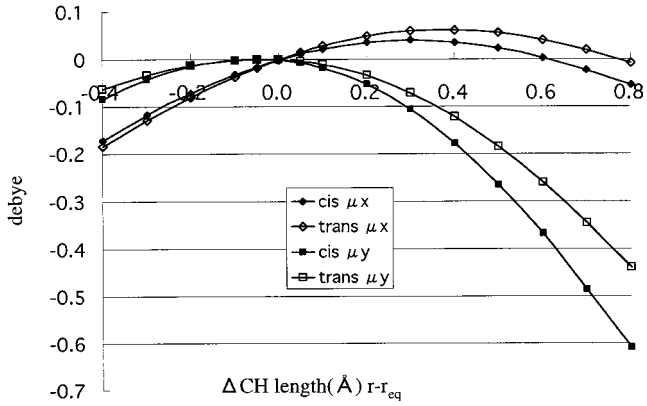

Figure 3. The gas-phase dipole moment function (B3PW91/aug-cc-pVTZ), both *x* and *y* components, given in debye. The cis isomer values are shaded, while the trans isomer values are open. The rhombuses are for the *x* component, while the squares are for the *y* component.

TABLE 2: Mulliken Charge on the Atoms of 1,2-Dichloroethylene at Optimized Geometry

	B3PW91			B3LYP	
	cis gas	trans gas	cis liq	cis gas	trans gas
C	−0.205	−0.208	−0.200	−0.225	−0.235
H	+0.365	+0.419	+0.369	+0.347	+0.405
Cl	−0.160	−0.210	−0.168	−0.122	−0.171

Upon the optimization of the cis isomer with the SCRF method, we saw a 0.3 D increase in the dipole moment, namely, to 2.11 D, but as seen in Table 1, there was no significant change in the geometry. This is in accord with past calculations using this method.[15−17] Because of the dielectric continuum, the chlorine atom was stabilized with a more negative charge, while the opposite occurred for the hydrogen atom, as can be seen in Table 2. This led to the larger dipole moment.

3.2. Vibrational Calculation. The ab initio PES and DMF used for the vibrational calculation are given in Figures 2 and 3, respectively. Because all of the vibration calculation results were very similar for both phases and both functionals, we will only show the results of the gas-phase calculation using B3PW91. In Figure 4, we show the calculated vibrational wave function along with the PES of the gas-phase calculation using the B3PW91 functional. Here, we can see that the range used in the present calculation, $r_{eq} - 0.5$ to $r_{eq} + 0.8$, was wide

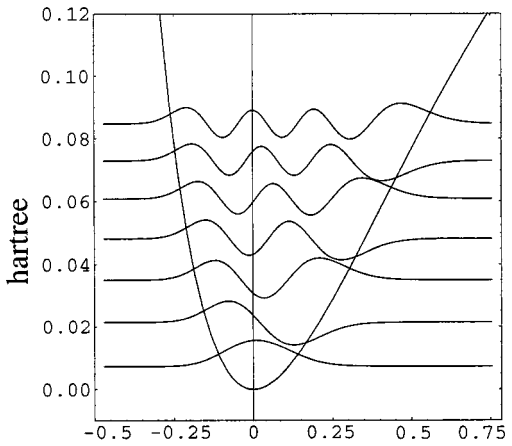

(a)

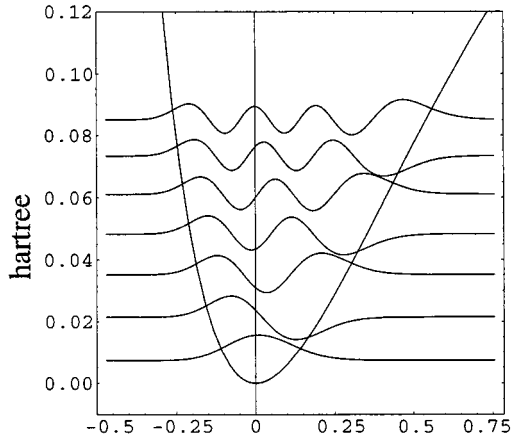

(b)

Figure 4. The vibration wave functions along with the potential energy curve of gas phase (a) *cis*- and (b) *trans*-dichloroethylene calculated with the B3PW91 functional.

enough for the calculation of the wave functions up to the $v = 6$ state. Moreover, vibrational calculation using additional data of $r_{eq} + 0.9$ and $r_{eq} + 1.0$ and increasing the grid points to $r_{eq} + 1.0$ did not change the results.

For comparison, we use the gas-phase experimental results[47,48] for the fundamental transition and the aforementioned liquid results[11] for overtones. The experimental value for the 0-3 CH stretching overtone is not available due to the coupling with the combination band of 0-2 CH stretching and CH bending and CC stretching.[11]

The calculated results together with the experimental data for the vibrational transition energy are shown in Table 3. One can notice that the calculated values for each transition are nearly identical for both the two phases and the two isomers. In both phases, the calculated transition energies of the trans isomer are slightly greater than the ones of the cis isomer. This is in accord with Henry's bond length frequency correlation,[49] where the shorter bond length of the trans isomer (Table 1) is expected to correspond to the higher frequency CH stretching oscillator. In comparison with experimental values, we see that for both isomers and for every overtone state the difference is about 1%.

TABLE 3: Vibrational Transition Energy ($v \leftarrow 0$) in cm^{-1}

	B3PW91				B3LYP		
v	cis gas	trans gas	cis liq	trans liq	cis gas	trans gas	exptl
1	3 102	3 111	3 104	3 111	3 096	3 107	3 087,[a] 3 090[b]
2	6 095	6 113	6 100	6 113	6 081	6 103	6 050[c]
3	8 980	9 009	8 988	9 009	8 955	8 990	
4	11 760	11 801	11 782	11 801	11 722	11 772	11 600[c]
5	14 437	14 490	14 452	14 490	14 385	14 450	14 203[c]
6	17 014	17 080	17 033	17 080	16 946	17 027	16 694[c]

[a] Experimental results for gas-phase cis isomer from ref 47. [b] Experimental results for gas-phase trans isomer from ref 48. [c] Experimental results for liquid phase from ref 11.

TABLE 4: Integrated Absorption Coefficient (km/mol) of $v \leftarrow 0$ Transition

Cis Isomer

	B3PW91			B3LYP	
v	gas	liq	liq/gas[a]	gas	exptl
1	7.05	10.9	1.55	6.76	10.3 (gas)[b]
2	1.87	2.55	1.36	2.00	1.04[d]
3	1.21×10^{-1}	1.50×10^{-1}	1.24	1.30×10^{-1}	
4	7.71×10^{-3}	9.56×10^{-3}	1.24	8.58×10^{-3}	7.87×10^{-3}[d]
5	6.95×10^{-4}	8.45×10^{-4}	1.22	8.88×10^{-4}	7.71×10^{-4}[d]
6	1.03×10^{-4}	1.41×10^{-4}	1.37	1.56×10^{-4}	7.37×10^{-5}[d]

Trans Isomer

	B3PW91			B3LYP	
v	gas	liq	liq/gas[a]	gas	exptl
1	8.87	11.0	1.24	8.56	10.5 (gas)[c]
2	1.43	1.63	1.14	1.52	6.77×10^{-1}[d]
3	7.55×10^{-2}	8.45×10^{-2}	1.12	8.19×10^{-2}	
4	4.48×10^{-3}	4.94×10^{-3}	1.10	5.13×10^{-3}	4.44×10^{-3}[d]
5	4.36×10^{-4}	5.41×10^{-4}	1.24	5.27×10^{-4}	4.12×10^{-4}[d]
6	7.34×10^{-5}	1.38×10^{-4}	1.88	6.21×10^{-5}	4.84×10^{-5}[d]

[a] Ratio between the liquid- and gas-phase calculation results. [b] Experimental results for gas-phase cis isomer from ref 47. [c] Experimental results for gas-phase trans isomer from ref 48. [d] Experimental results for liquid phase from ref 11.

This can also be seen from the Birge−Sponer relationship in cm^{-1}:

$$E_{v0}/v = 3153.0 - 53.0v \quad \text{(cis calcd gas)} \quad (29)$$

$$E_{v0}/v = 3154.9 - 52.8v \quad \text{(cis calcd liq)} \quad (30)$$

$$E_{v0}/v = 3145.4 - 60.8v \quad \text{(cis exptl liq)} \quad (31)$$

$$E_{v0}/v = 3161.3 - 52.6v \quad \text{(trans calcd gas)} \quad (32)$$

$$E_{v0}/v = 3161.3 - 52.6v \quad \text{(trans calcd liq)} \quad (33)$$

$$E_{v0}/v = 3149.6 - 61.4v \quad \text{(trans exptl liq).} \quad (34)$$

The deviation from experimental values is on the order of 10 cm^{-1}.

Next, we compare the integrated absorption coefficients in Table 4. First, as for the fundamental in the gas phase, the experimental integrated absorption coefficients of cis and trans isomers have been reported to be 10.3[47] and 10.5,[48] respectively. As seen in Tables 4 and 5, the calculated intensity for both isomers in the simple local mode model underestimates this, and the ratio between the two isomers also shows some error. Calculation under the normal coordinates and harmonic approximation for the DMF gave values of 16.1 and 15.7 for cis

TABLE 5: Integrated Absorption Coefficient Ratio cis/trans

	B3PW91		B3LYP	
ν	gas	liq	gas	exptl
1	0.80	0.99	0.79	0.98 (gas)[a,b]
2	1.31	1.56	1.31	1.53[c]
3	1.60	1.78	1.59	
4	1.72	1.93	1.67	1.77[c]
5	1.59	1.56	1.69	1.87[c]
6	1.40	1.02	2.50	1.52[c]

[a] Experimental results for gas-phase cis isomer from ref 47. [b] Experimental results for gas-phase trans isomer from ref 48. [c] Experimental results for liquid phase from ref 11.

TABLE 6: Integrated Absorption Coefficient Ratio Calcd/Exptl (liquid phase)

	B3PW91				B3LYP	
ν	cis gas	trans gas	cis liq	trans liq	cis gas	trans gas
2	1.80	2.11	2.46	2.41	1.92	2.25
4	0.98	1.01	1.21	1.11	1.09	1.16
5	0.90	1.06	1.10	1.31	1.15	1.28
6	1.39	1.52	1.90	2.86	2.11	1.28

and trans isomers, respectively. Though it overestimated the absolute value, the ratio between the two isomers was in good agreement with the experimental value. From this, we can attribute the difference in the ratio to the use of local mode coordinates, instead of the normal coordinates, for the fundamental transition. The ratio between the calculated and the liquid-phase experimental[11] integrated absorption coefficient for the overtones is listed in Table 6. As seen here, for the 0-2 transition, the calculated value overestimates the intensity by a factor of 2 for both isomers, probably because of the same reason as for the fundamental. Though a slight deviation is seen in the 0-6 transition for the trans isomer, a good agreement is obtained for the transitions 0-4, 0-5, and 0-6.

Next, we discuss the liquid-phase calculation. With the local mode model, the transition energies show little deviation from the gas-phase calculation; however, the intensity is increased by a factor of 1.55 and 1.24 for the fundamental of the cis and trans isomer, respectively (Table 4, column 4). This factor under the normal mode model was 1.66 and 1.25, for cis and trans isomer, respectively. As can be noticed, this absorption intensity ratio between the two phases does not depend on the model of the vibrational calculation, namely, local or normal mode model. Thereby, the ratio is mainly due to the SCRF effect. Considering that the reaction field acts on the molecule with dipole moment, it is logical that the difference between the two phases is greater for the cis isomer. Comparison with several semiclassical formulas for the ratio of the absorption intensities in the solution and gas phase[18,50,51] of the fundamental vibration suggests that the present calculation overestimated this ratio. For example, Hirota's formula[50] is given as

$$\frac{A_{s01}}{A_{g01}} = \frac{(n^2+2)(2\epsilon+1)}{3(n^2+2\epsilon)} \tag{35}$$

where A_{s01} and A_{g01} are the fundamental absorption intensity in solution and gas, respectively, and n is the refractive index of the solute. Another formula proposed by Buckingham[51] is

$$\frac{A_{s01}}{A_{g01}} = \frac{9n^2}{(n^2+2)(2n^2+1)}\left[\frac{(n^2+2)(2\epsilon+1)}{3(n^2+2\epsilon)}\right] \tag{36}$$

Using the values n(cis) = 1.4490[41] and n(trans) = 1.4454,[41] we obtained the ratios of 1.29 and 1.13, respectively, using Hirota's formula and 1.15 and 1.01 using Buckingham's formula. Further SCRF calculations varying the cavity radius revealed that increasing the cavity radius causes this calculated intensity ratio between the two phases to decrease. From the results of the present calculation, we can say that the SCRF method using the cavity radius given by the VOLUME keyword tends to overestimate the absorption intensity of the fundamental in solution. As for the overtones, one can notice a general feature that the ratios between the two phases are smaller than the ones of the fundamental (Table 4, column 4). This suggests that the overtone intensities may not be as sensitive to the phase as the fundamental intensities, at least in the liquid and gas phases.

Finally, comparison on the cis versus trans ratio of the integrated absorption coefficients of the overtones will be given. Because there are uncertainties concerning the liquid-phase calculations, as mentioned above, the gas-phase results will be used for the following discussion. As discussed earlier, the absorption intensity depends on both the vibrational wave function and the DMF. From the similarities in the PES, as shown in Figure 2, and in the eigenvalues of each vibrational state, 0 to 6, the vibrational wave functions of the two isomers can be regarded as nearly identical. As a proof, the calculated overlap between the corresponding υ quantum wave functions of the two isomers was found to deviate from unity by less than 10^{-4}. Thereby, the difference in intensities between the two isomers is due to the difference in the DMF. From the examination of the transition moments, listed in Table 7, it can be seen that the greater difference between the isomers is in the y component. Looking at Figure 3, one can easily notice that the y component DMF for both isomers is distorted from a linear function. By fitting the 16 ab initio single-point results onto a polynomial of bond displacement, R ($R = r - r_{eq}$ in bohr), using the "Fit[data, function]" function built in the *Mathematica* program, we obtained the following:

$$\mu_y(\text{cis}) \cong \mu_y(\text{cis},r_{eq}) - (4.38\times10^{-2})R - (2.27\times10^{-1})R^2 - (4.53\times10^{-2})R^3 + (5.33\times10^{-3})R^4 + (2.43\times10^{-2})R^5 - (7.16\times10^{-3})R^6 \tag{37}$$

$$\mu_y(\text{trans}) \cong -(2.24\times10^{-2})R - (1.59\times10^{-1})R^2 - (3.82\times10^{-2})R^3 + (1.23\times10^{-3})R^4 + (1.78\times10^{-2})R^5 - (4.85\times10^{-3})R^6 \tag{38}$$

Using these results and the matrix element of $\langle 0|R^n|\upsilon\rangle$, where the $|\upsilon\rangle$ denotes the υ-th vibrational wave function, we divided the y transition moment into each component of the C_nR^n term, where C_n is the coefficient of the R^n term in eqs 37 and 38. The integrated values of $C_n\langle 0|R^n|\upsilon\rangle$ are listed in Table 8. It was found that for an accurate calculation of the transition moment of the fifth overtone, terms as high as the fifth term were inevitable. Further investigation shows that the main contribution for the overtone intensity is from the first three terms. As seen in Table 8, the values, $C_n\langle 0|R^n|\upsilon\rangle$, of the R^1 and R^3 terms have the sign opposite to the ones of the R^2 term, especially for $\upsilon \geq 3$. Because the coefficients C_n for the first three terms have the same negative sign in eqs 37 and 38, the above feature is due to the difference in the sign of the $\langle 0|R^n|\upsilon\rangle$. In the y transition moment, the positive contribution of the R^2 term is much greater than the negative cancellations of the R^1 and R^3 terms. Because $\langle 0|R^2|\upsilon\rangle$ is almost identical for the two isomers with similar PES, the absolute values of the coefficient of the R^2 term, C_2, should be compared. As seen from the above equations, the cis isomer has a greater absolute value. We conclude that the absorption

TABLE 7: The Transition Moments (D) of $v \leftarrow 0$ Transition[a]

Cis Isomer

	B3PW91 gas		B3PW91 gas		B3PW91 liq		B3LYP gas	
v	x	y	x (lsq)[b]	y (lsq)[b]	x	y	x	y
1	2.66×10^{-2}	1.41×10^{-2}	2.66×10^{-2}	1.43×10^{-2}	3.71×10^{-2}	5.74×10^{-3}	2.56×10^{-2}	1.47×10^{-2}
2	7.55×10^{-3}	8.09×10^{-3}	7.55×10^{-3}	8.08×10^{-3}	8.99×10^{-3}	9.26×10^{-3}	7.76×10^{-3}	8.41×10^{-3}
3	1.53×10^{-3}	1.74×10^{-3}	1.50×10^{-3}	1.73×10^{-3}	1.74×10^{-3}	1.91×10^{-3}	1.57×10^{-3}	1.82×10^{-3}
4	3.48×10^{-4}	3.75×10^{-4}	3.54×10^{-4}	3.95×10^{-4}	3.93×10^{-4}	4.12×10^{-4}	3.68×10^{-4}	3.96×10^{-4}
5	9.08×10^{-5}	1.05×10^{-4}	1.06×10^{-4}	1.20×10^{-4}	1.14×10^{-4}	1.01×10^{-4}	1.13×10^{-4}	1.09×10^{-4}
6	2.60×10^{-5}	4.16×10^{-5}	3.92×10^{-5}	4.55×10^{-5}	4.48×10^{-5}	3.58×10^{-5}	4.02×10^{-5}	4.53×10^{-5}

Trans Isomer

	B3PW91 gas		B3PW91 gas		B3PW91 liq		B3LYP gas	
v	x	y	x (lsq)[b]	y (lsq)[b]	x	y	x	y
1	3.27×10^{-2}	8.34×10^{-3}	3.27×10^{-2}	8.30×10^{-3}	3.62×10^{-2}	1.00×10^{-2}	3.22×10^{-2}	7.71×10^{-3}
2	7.69×10^{-3}	5.84×10^{-3}	7.72×10^{-3}	5.88×10^{-3}	8.29×10^{-3}	6.15×10^{-3}	7.93×10^{-3}	6.04×10^{-3}
3	1.40×10^{-3}	1.18×10^{-3}	1.43×10^{-3}	1.18×10^{-3}	1.50×10^{-3}	1.22×10^{-3}	1.48×10^{-3}	1.20×10^{-3}
4	2.96×10^{-4}	2.53×10^{-4}	3.22×10^{-4}	2.62×10^{-4}	3.25×10^{-4}	2.47×10^{-4}	3.24×10^{-4}	2.63×10^{-4}
5	8.44×10^{-5}	6.99×10^{-5}	9.53×10^{-5}	7.92×10^{-5}	1.04×10^{-4}	6.34×10^{-5}	8.63×10^{-5}	8.43×10^{-5}
6	3.52×10^{-5}	2.18×10^{-5}	3.52×10^{-5}	3.04×10^{-5}	4.79×10^{-5}	3.04×10^{-5}	2.56×10^{-5}	2.83×10^{-5}

[a] All of the transition moments, except for the columns 4 and 5, were calculated from the potential energy surface and dipole moment function obtained by interpolation. [b] Calculated from the potential energy surface obtained by fitting to power series expansion of the Morse function and from the dipole moment function obtained by fitting to a polynomial of bond displacement.

TABLE 8: Division of the *y* Transition Moments (D) of the Gas-Phase Calculation into Their Dependence on the Harmonic and Anharmonic Terms of the Dipole Moment Function (Using Values Obtained by Fitting 16 ab Initio Single Point Calculations)

Cis Isomer

v	r^1	r^2	r^3	r^4	r^5	r^6	sum(r^1−r^6)[a]
1	8.86×10^{-3}	4.75×10^{-3}	6.53×10^{-4}	-1.65×10^{-5}	-4.36×10^{-5}	4.17×10^{-6}	1.42×10^{-2}
2	-8.98×10^{-4}	8.67×10^{-3}	3.32×10^{-4}	-3.28×10^{-5}	-4.95×10^{-5}	9.23×10^{-6}	8.03×10^{-3}
3	-1.59×10^{-4}	2.17×10^{-3}	-3.55×10^{-4}	1.13×10^{-5}	5.98×10^{-5}	-8.07×10^{-6}	1.72×10^{-3}
4	-3.75×10^{-5}	5.97×10^{-4}	-1.63×10^{-4}	-8.22×10^{-6}	-1.03×10^{-5}	6.45×10^{-6}	3.84×10^{-4}
5	-1.07×10^{-5}	1.87×10^{-4}	-6.41×10^{-5}	-6.51×10^{-6}	6.80×10^{-6}	1.51×10^{-7}	1.13×10^{-4}
6	-3.55×10^{-6}	6.52×10^{-5}	-2.56×10^{-5}	-3.50×10^{-6}	9.28×10^{-6}	4.41×10^{-7}	4.23×10^{-5}

Trans Isomer

v	r^1	r^2	r^3	r^4	r^5	r^6	sum(r^1−r^6)[a]
1	4.53×10^{-3}	3.31×10^{-3}	5.46×10^{-4}	-3.77×10^{-6}	-3.17×10^{-5}	2.80×10^{-6}	8.35×10^{-3}
2	-4.56×10^{-4}	6.07×10^{-3}	2.79×10^{-4}	-7.51×10^{-6}	-3.60×10^{-5}	6.19×10^{-6}	5.86×10^{-3}
3	-8.05×10^{-5}	1.51×10^{-3}	-2.99×10^{-4}	2.59×10^{-6}	4.35×10^{-5}	-5.40×10^{-6}	1.17×10^{-3}
4	-1.90×10^{-5}	4.14×10^{-4}	-1.37×10^{-4}	-1.91×10^{-6}	-7.50×10^{-6}	4.33×10^{-6}	2.53×10^{-4}
5	-5.42×10^{-6}	1.29×10^{-4}	-5.31×10^{-5}	-1.49×10^{-6}	5.01×10^{-6}	9.33×10^{-8}	7.44×10^{-5}
6	-1.79×10^{-6}	4.50×10^{-5}	-2.12×10^{-5}	-8.00×10^{-7}	6.75×10^{-6}	3.02×10^{-7}	2.82×10^{-5}

[a] Sum of the values of the six terms.

difference between the two isomers originates from the difference in the first anharmonic term, the R^2 term, of the y component DMF.

3.3. Computational Efficiency and Accuracy. We were able to calculate the CH stretching overtone absorption intensity of *cis*- and *trans*-dichloroethylene with high accuracy by using a simple local mode model in which only the motion of one hydrogen atom was considered. This is attributed to (1) the applicability of the local mode picture in describing light−heavy overtone vibrations and (2) the high accuracy of the theoretical calculation. An important, but often neglected, aspect upon considering the accuracy of the theoretical vibrational calculation is the proper incorporation of the ab initio results, in the shape of PES and DMF.

For the calculation of the CH stretching overtone spectra of naphthalene cations, Kjaergaard et al. obtained their PES in a Morse potential form by calculating the Morse parameters using the ab initio force constant expansion around the equilibrium region.[7] As for the DMF, they used the Taylor series expansion using ab initio values calculated around the equilibrium bond length. Although the accuracy of the expansion is limited to the neighborhood of the equilibrium bond length, their success with this method[5−7] suggests that their simple approximation may be sufficient in obtaining the general behavior of the actual PES and DMF even in regions far from the equilibrium. However, for an accurate high-energy vibrational calculation, precise data on the PES and the DMF in regions far from equilibrium are expected to be important.

In most higher-energy vibrational calculations, the ab initio results are fitted to analytical functions and the Schrödinger equation is solved variationally by the basis set expansion method. Because a high-order polynomial tends to lead to a fitted function that oscillates in the region between the sampling points, it is not suitable for the description of the PES and DMF. In the present work, we derived both the PES and DMF by sixth-order divided difference interpolation of the 16 ab initio single-point results. In this method, unlike fitting, where one function is used for all regions, the interpolated function is constructed by connecting locally defined functions at the interval of sample points. Each locally defined function, a sixth-order polynomial, is chosen to match the sample point values at six points adjacent to the interval. Therefore, we are able to

construct a function that passes through all 16 sample points without using a fifteenth-order polynomial, which would be needed if constructed from the least-squares fit. These features cause the resulting interpolated function to be smooth and precise, as will be discussed.

In the following, we will examine the accuracy of the PES and DMF depending on the method of data incorporation, namely, interpolation or least-squares fit. Ideally, the PES and DMF are expected to reproduce the ab initio results at every bond length. Comparing the values at the 16 sample points mentioned before and the values calculated additionally at 10 bond lengths ($r_{eq} \pm 0.15$, 0.25, 0.35, and 0.45 and $r_{eq} + 0.55$ and 0.65), we obtained standard deviations of 1.60×10^{-5} hartree (3.51 cm^{-1}) and 1.58×10^{-5} hartree (3.47 cm^{-1}) for our interpolated PES of the cis and trans isomer, respectively. Because fitting the 16 ab initio potential energy data to a sixth-power series of Morse function $f(R) = \exp(-\alpha R)$, where $\alpha = \omega_e\sqrt{m/(2D_e)} = 1.04$ and R is the displacement coordinate, gave much smoother potential functions than the fit to a sixth-order polynomial of R, the former will be used for the following discussion. By using the "Fit[data, function]" function built in the *Mathematica* program, we obtained

$$V(\text{cis}) \cong V(\text{cis},r_{eq}) + 0.2164 - 0.5642f(R) + 0.5960f^2(R) - 0.4056f^3(R) + 0.2047f^4(R) - 0.052\,70f^5(R) + 0.005\,604f^6(R) \quad (39)$$

and

$$V(\text{trans}) \cong V(\text{trans},r_{eq}) + 0.2192 - 0.5753f(R) + 0.6147f^2(R) - 0.4231f^3(R) + 0.2138f^4(R) - 0.055\,17f^5(R) + 0.005\,872f^6(R) \quad (40)$$

The standard deviations compared at the 26 points, mentioned above, were 2.18×10^{-4} hartree (47.8 cm^{-1}) and 2.30×10^{-4} hartree (50.5 cm^{-1}) for the cis and trans isomers, respectively.

As for the dipole moment, we will compare the accuracy of our interpolated DMF and the sixth-order polynomial of R obtained by fitting the 16 ab initio sample point results, namely, eqs 37 and 38, for the y component and the following for the x component:

$$\mu_x(\text{cis}) \cong (1.45 \times 10^{-1})R - (1.15 \times 10^{-1})R^2 - (2.35 \times 10^{-2})R^3 + (1.95 \times 10^{-3})R^4 + (1.60 \times 10^{-2})R^5 - (5.41 \times 10^{-3})R^6 \quad (41)$$

$$\mu_x(\text{trans}) \cong (1.74 \times 10^{-1})R - (1.03 \times 10^{-1})R^2 - (3.02 \times 10^{-2})R^3 + (3.60 \times 10^{-4})R^4 + (1.71 \times 10^{-2})R^5 - (5.53 \times 10^{-3})R^6 \quad (42)$$

For the cis isomer, while our interpolated DMF had standard deviations of 2.83×10^{-5} and 2.00×10^{-5} D from the ab initio values for the x and y components, respectively, the polynomial expansion resulted in larger standard deviations of 3.32×10^{-4} and 3.02×10^{-4} D. For the trans isomer, the interpolated DMF, once again, had smaller standard deviations of 5.66×10^{-5} and 4.00×10^{-5} D compared to 1.64×10^{-4} and 3.38×10^{-4} D of the fitted polynomial for the x and y components, respectively. The standard deviation of the interpolated function was 1 order of magnitude smaller than that of the least-squares fitted function. However, the accuracy of this powerful divided difference interpolation method is limited to the range of the sample data. Thus, we used the grid method in the vibrational calculation and only considered the region where the ab initio data are available.

To see the sensitivity of the final results to the choice of the data incorporation methods, in Table 7, the transition moments calculated by the least-squares fits, namely, the PES of eqs 39 and 40 and the DMF of eqs 37, 38, 41, and 42, are compared with those calculated by the interpolation method. It can be seen that the different method causes the transition moment of higher overtones to vary significantly. For example, as seen for the fifth overtone ($v = 6$), vibrational calculation using the fitting method, which is slightly inaccurate compared to interpolation, may contain relative error of about 50%. As a summary, our grid method, which employs the PES and DMF by sixth-order divided difference interpolation of the ab initio results, utilizes the ab initio data in an efficient and accurate manner upon incorporating them into the vibrational calculation. This is essential for the qualitative calculation of the intensity of higher overtones.

4. Conclusion

We have succeeded in reproducing the transition energy and the absorption intensity of the overtone CH stretching vibration of *cis*- and *trans*-dichloroethylene using the simple local mode model and the PES and DMF obtained from ab initio calculation. We were able to gain insight on the reason for the larger integrated absorption coefficient for the cis isomer in 1,2-dichloroethylene, namely, the DMF of the direction perpendicular to the CC bond is distorted from linearity and its distortion is larger in the cis isomer. As for the use of hybrid density functional theory method on elongated bond lengths, judging from the agreement in transition energies and absorption intensities, it can be said that an accurate PES and DMF were calculated. For further use of the present vibrational calculation method, computational efficiency and accuracy in representing the PES and DMF were discussed.

Acknowledgment. This work was supported in part by Research and Development Applying Advanced Computational Science and Technology, Japan Science and Technology Corporation, and by a Grants-in-Aid for Scientific Research from Ministry of Education, Science, Culture, and Sports of Japan. S.Y. would like to thank the late Professor Naoto Yamamoto, who died after having carried out the experimental measurement described in this paper, Mr. Yoshio Okada, and Prof. Hiroshi Tsubomura.

References and Notes

(1) Siebrand, W.; Williams, D. F. *J. Chem. Phys.* **1968**, *49*, 1860.
(2) Swofford, R. L.; Long, M. E.; Albrecht, A. C. *J. Chem. Phys.* **1976**, *65*, 179.
(3) Lawton, R. T.; Child, M. S. *Mol. Phys.* **1979**, *37*, 1799.
(4) Møller, H. S.; Sonnich Mortensen, O. *Chem. Phys. Lett.* **1979**, *66*, 539.
(5) Kjaergaard, H. G.; Goddard, J. D.; Henry, B. R. *J. Chem. Phys.* **1991**, *95*, 5556.
(6) Kjaergaard, H. G.; Daub, C. D.; Henry, B. R. *Mol. Phys.* **1997**, *90*, 201.
(7) Kjaergaard, H. G.; Robinson, T. W.; Brooking, K. A. *J. Phys. Chem. A* **2000**, *104*, 11297.
(8) Burberry, M. S.; Albrecht, A. C. *J. Chem. Phys.* **1979**, *71*, 4768.
(9) Yamamoto, N.; Sawada, T.; Tsubomura, H. *Bull. Chem. Soc. Jpn.* **1979**, *52*, 987.
(10) Yamamoto, N.; Matsuo, N.; Tsubomura, H. *Chem. Phys. Lett.* **1980**, *71*, 463.
(11) Okada, Y. Master Thesis, Osaka University, Japan, 1982.
(12) Yabushita, S. Doctor Thesis, Osaka University, Japan, 1982.

(13) Wright, N. J.; Gerber, R. B.; Tozer, D. J. *Chem. Phys. Lett.* **2000**, *324*, 206.
(14) Onsager, L. *J. Am. Chem. Soc.* **1936**, *58*, 1486.
(15) Wong, M. W.; Frisch, M. J.; Wiberg, K. B. *J. Am. Chem. Soc.* **1991**, *113*, 4776.
(16) Wong, M. W.; Wiberg, K. B.; Frisch, M. J. *J. Am. Chem. Soc.* **1992**, *114*, 523.
(17) Wong, M. W.; Wiberg, K. B.; Frisch, M. J. *J. Am. Chem. Soc.* **1992**, *114*, 1645.
(18) Cammi, R.; Cappelli, C.; Corni, S.; Tomasi, J. *J. Phys. Chem. A* **2000**, *104*, 9874.
(19) Low, G. R.; Kjaergaard, H. G. *J. Chem. Phys.* **1999**, *110*, 9104.
(20) Chýlek, P.; Geldart, D. J. W. *Geophys. Res. Lett.* **1997**, *24*, 2015.
(21) Lange, K. R.; Wells, N. P.; Plegge, K. S.; Phillips, J. A. *J. Phys. Chem. A* **2001**, *105*, 3481.
(22) Lin, H.; Yuan, L.-F.; He, S.-G.; Wang, X.-G. *J. Chem. Phys.* **2001**, *114*, 8905.
(23) Lin, H.; Bürger, H.; Mkadmi, E. B.; He, S.-G.; Yuan, L.-F.; Breidung, J.; Thiel, W.; Huet, T. R.; Demaison, J. *J. Chem. Phys.* **2001**, *115*, 1378.
(24) Gelbart, W. M.; Stannard, P. R.; Elert, M. L. *Int. J. Quantum Chem.* **1978**, *14*, 703.
(25) McCullough, E. A., Jr.; Wyatt, R. E. *J. Chem. Phys.* **1971**, *54*, 3578.
(26) Cerjan, C.; Kulander, K. C. *Comput. Phys. Commun.* **1991**, *63*, 529.
(27) Sugawara, M.; Kato, M.; Fujimura, Y. *Chem. Phys. Lett.* **1991**, *184*, 203.
(28) Skeel, R. D.; Keiper, J. D. *Elementary Numerical Computing with Mathematica*; McGraw-Hill: New York, 1993; Chapter 5.
(29) Atkinson, K. *Elementary Numerical Analysis*; John Wiley and Sons: New York, 1985; Chapter 5.
(30) Frisch, M. J.; Trucks, G. W.; Schlegel, H. B.; Scuseria, G. E.; Robb, M. A.; Cheeseman, J. R.; Zakrzewski, V. G.; Montgomery, J. A., Jr.; Stratmann, R. E.; Burant, J. C.; Dapprich, S.; Millam, J. M.; Daniels, A. D.; Kudin, K. N.; Strain, M. C.; Farkas, O.; Tomasi, J.; Barone, V.; Cossi, M.; Cammi, R.; Mennucci, B.; Pomelli, C.; Adamo, C.; Clifford, S.; Ochterski, J.; Petersson, G. A.; Ayala, P. Y.; Cui, Q.; Morokuma, K.; Malick, D. K.; Rabuck, A. D.; Raghavachari, K.; Foresman, J. B.; Cioslowski, J.; Ortiz, J. V.; Stefanov, B. B.; Liu, G.; Liashenko, A.; Piskorz, P.; Komaromi, I.; Gomperts, R.; Martin, R. L.; Fox, D. J.; Keith, T.; Al-Laham, M. A.; Peng, C. Y.; Nanayakkara, A.; Gonzalez, C.; Challacombe, M.; Gill, P. M. W.; Johnson, B. G.; Chen, W.; Wong, M. W.; Andres, J. L.; Head-Gordon, M.; Replogle, E. S.; Pople, J. A. *Gaussian 98*, revision A.5; Gaussian, Inc.: Pittsburgh, PA, 1998.
(31) Becke, A. D. *J. Chem. Phys.* **1993**, *98*, 5648.
(32) Perdew, J. P.; Chevary, J. A.; Vosko, S. H.; Jackson, K. A.; Pederson, M. R.; Singh, D. J.; Fiolhais, C. *Phys. Rev. B* **1992**, *46*, 6671.
(33) Lee, C.; Yang, W.; Parr, R. G. *Phys. Rev. B* **1988**, *37*, 785.
(34) Woon, D. E.; Dunning, T. H., Jr. *J. Chem. Phys.* **1993**, *98*, 1358.
(35) Kendall, R. A.; Dunning, T. H., Jr.; Harrison, R. J. *J. Chem. Phys.* **1992**, *96*, 6796.
(36) Dunning, T. H., Jr. *J. Chem. Phys.* **1989**, *90*, 1007.
(37) Ditchfield, R.; Hehre, W. J.; Pople, J. A. *J. Chem. Phys.* **1971**, *54*, 724.
(38) Frisch, M. J.; Pople, J. A.; Binkley, J. S. *J. Chem. Phys.* **1984**, *80*, 3265.
(39) McLean, A. D.; Chandler, G. S. *J. Chem. Phys.* **1980**, *72*, 5639.
(40) Krishnan, R.; Binkley, J. S.; Seeger, R.; Pople, J. A. *J. Chem. Phys.* **1980**, *72*, 650.
(41) *CRC Handbook of Chemistry and Physics*, 79th ed.; CRC Press: New York, 1998.
(42) Schäfer, L.; Ewbank, J. D.; Siam, K.; Paul, D. W.; Monts, D. L. *J. Mol. Struct.* **1986**, *145*, 135.
(43) Takeo, H.; Sugie, M.; Matsumura, C. *J. Mol. Struct.* **1988**, *190*, 205.
(44) Craig, N. C.; Appleman, R. A.; Barnes, H. E.; Morales, E.; Smith, J. A.; Klee, S.; Lock, M.; Mellau, G. C. *J. Phys. Chem. A* **1998**, *102*, 6745.
(45) Craig, N. C.; Piper, L. G.; Wheeler, V. L. *J. Phys. Chem.* **1971**, *75*, 1453.
(46) Bingham, R. C. *J. Am. Chem. Soc.* **1976**, *98*, 535.
(47) Hopper, M. J.; Overend, J.; Ramos, M. N.; Bassi, A. B. M. S.; Bruns, R. E. *J. Chem. Phys.* **1983**, *79*, 19.
(48) Kagel, R. O.; Powell, D. L.; Hopper, M. J.; Overend, J.; Ramos, M. N.; Bassi, A. B. M. S.; Bruns, R. E. *J. Phys. Chem.* **1984**, *88*, 521.
(49) Henry, B. R. *Acc. Chem. Res.* **1987**, *20*, 429.
(50) Hirota, E. *Bull. Chem. Soc. Jpn.* **1954**, *27*, 295.
(51) Buckingham, A. D. *Proc. R. Soc. London* **1958**, *A248*, 169.